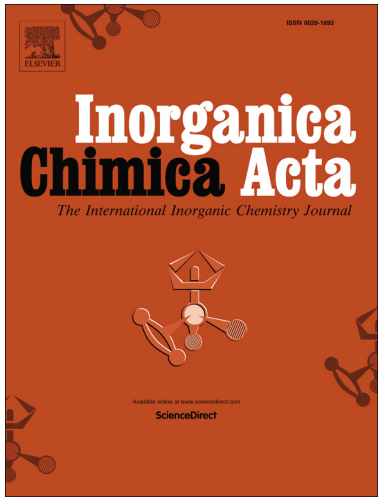

Research paper

Complexation of trichlorosalicylic acids by alkaline and first row transition metals as a switch for their antibacterial activity

Vijay Kumar, Mohit Chawla, Luigi Cavallo, Abdul Basit Wani, Anu Manhas, Sukhmanpreet Kaur, Albert Poater, Hemlata Chadar, NirajUpadhyay

PII: S0020-1693(17)30859-9
DOI: http://dx.doi.org/10.1016/j.ica.2017.08.064
Reference: ICA 17884

To appear in: *Inorganica Chimica Acta*

Received Date: 1 June 2017
Revised Date: 25 August 2017
Accepted Date: 26 August 2017

Please cite this article as: V. Kumar, M. Chawla, L. Cavallo, A. Basit Wani, A. Manhas, S. Kaur, A. Poater, H. Chadar, NirajUpadhyay, Complexation of trichlorosalicylic acids by alkaline and first row transition metals as a switch for their antibacterial activity, *Inorganica Chimica Acta* (2017), doi: http://dx.doi.org/10.1016/j.ica.2017.08.064

Complexation of trichlorosalicylic acids by alkaline and first row transition metals as a switch for their antibacterial activity

Vijay Kumar,[a,b] Mohit Chawla,[c] Luigi Cavallo,[c] Abdul Basit Wani,[a] Anu Manhas,[a,d] Sukhmanpreet Kaur,[a] Albert Poater,[c,e] Hemlata Chadar,[f] and NirajUpadhyay*[f]

[a.] *Department of Chemistry, School of Sciences, Lovely Professional University, Jalandhar*, India.
[b.] *Regional Ayurveda Research Institute of Drug Development, Gwalior, India.*
[c.] *Department of Physical Science and Engineering, KAUST Catalysis Center, King Abdullah University of Science and Technology, Saudi Arabia.*
[d.] *School of Chemical Sciences, Central University of Gujarat, Gujarat, India.*
[e.] *Institut de Química Computacionali Catàlisi and Departament de Química, Universitat de Girona, Campus Montilivi, 17071 Girona, Catalonia, Spain.*
[f.] *Department of Chemistry, Dr. Harisingh Gour University, Madhya Pradesh, India.*

*Dr. Niraj Upadhyay
E- mail: nirajiitr@gmail.com

Abstract:

3,5,6-trichlorosalicylic acid (TCSA) does not show a good antibacterial activity. In contrast, here metal complexes with TCSA have shown better antibacterial activity for selected bacterial strains with a good degree of selectivity. Amongst the eight synthesized essential metal complexes complexed with TCSA, Mn(II)-TCSA and Ni(II)-TCSA have been found to be more effective with MIC range 20-50 µg/L as compared to control (chloramphenicol). The activity of an individual complex against different microbes was not found to be identical, indicating the usage of an individual metal chelate against a targeted bacterial strain. Further, the protein (BSA) binding constant of TCSA and its metal complexes were determined and ordered as Ca(II)-TCSA > Cu(II)-TCSA > Mg(II)-TCSA >> Mn(II)-TCSA >> Zn(II)-TCSA >>> Ni(II)-TCSA >>> Co(II)-TCSA > Fe(II)-TCSA > TCSA. The present study has confirmed enhanced antibacterial activities and binding constants for metal chelates of TCSA as compared to free TCSA, which seems directly related with the antioxidant activities of these complexes. Further, bearing the ambiguity related to the structural characterization of the metal complexed with TCSA ligands, DFT calculations have been used as the tool to unravel the right environment around the metals, studying basically the relative stability of square planar and octahedral metal complexes with TCSA.

Keywords: Trichlorosalicylic acid, divalent essential metal complexes, antibacterial activity, DFT calculation, BSA protein binding.

1. Introduction

The increase in the pathogen infections coupled with their associated resistance have motivated scientific community to develop novel drugs like compounds that may be more effective, with improved protein binding ability as compared to the already existing drugs. In this context, salicylic acid (SA) and its derivatives, as well as their metal complexes have gained much attention because of its associated pharmaceutical activities (Perrin, 1958; Hallmen et al., 1995, Wani et al. 2017a). In few cases, it has been noticed that the drug activity increases, when SA is administered as metal chelates, for instance in the inhibition of the growth of tumor cells (Brumas, 1995; Brumas, 2007 and Wani et al. 2017b). Quoting an example, the mono and di-substituted chloro-derivatives of salicylic acid have been shown to be biologically active (Kantouch et al. 2013 and Shi et al. 2007). In relation to its interaction with proteins, it has been observed that the SA and its derivatives possess low to medium covalent interaction with proteins like human serum albumin (HSA) and bovine serum albumin (BSA) (Kumar et al. 2015a; Yin et al. 2007 and Li et al. 2011), that is known to be one of the most abundant proteins in blood and cerebrospinal fluid, playing a fundamental role in the distribution of essential transition metal ions across different parts of the human body. The use of metal complexes as drugs requires transportation of the metal ion in the body which is achieved by the formation of non-covalent coordination of the drugs with its targeted protein, particularly utilizing the amino acid side chains (Archibald et al. 2013, Kaur et al. 2017).

In particular, 3,5,6-Trichlorosalicylic acid (TCSA) is a tri-substituted chlorinated salicylic acid derivative, which has a tendency to act as chelating agent utilizing the carbonyl and hydroxyl oxygens under erratic pH conditions. A single study reported by Wang et al. (2013) shows the formation of cage like complexes utilizing TCSA as ligand, and tin as a metal. To the best of our knowledge, we are the first to report the synthesis, characterization and stability studies of the TCSA complexes with different metal ions, such as Mg(II), Ca(II), Mn(II), Fe(II), Co(II), Ni(II), Cu(II) and Zn(II) at a physiological pH. Further, the biological activities like antibacterial activities and binding ability with BSA protein of these complexes have also been analyzed and reported in the present study.

2. Materials and Methods

2.1. Chemical Studies

2.1.1. Chemicals and instruments used

All the chemicals were of AR grade and purchased from Loba Chemie-India. All the microorganisms/ strains were purchased from NCL Pune-India with unique identity number. UV-Visible spectra were recorded in methanol/ DMSO (wherever applicable) with concentration (1.0×10^{-4} M) for the free ligands and their complexes using a Shimadzu-1800s at Lovely Professional University. Infrared spectra were collected on a Shimadzu-8400s in a working range of 4000 – 400 cm^{-1} in dry KBr pellets at Lovely Professional University. Mass (Waters, Q-TOF Micromass) and NMR spectra (in DMSO-d_6 and TMS as internal reference) were recorded on Bruker Avance III, 400MHz FT-NMR spectrometers at the SAIF Chandigarh, Chandigarh University. SEM (JEOL Model JSM - 6390LV) and TGA (Perkin Elmer STA 6000) were collected from University of Coachi (Kerala).

2.1.2. Synthesis procedure

10 mL aqueous solution of metal salt (1.0 mM) was added to a 10 mL methanolic solution of TCSA (2.0 mM), the pH of reaction mixture was adjusted at ~7 using 5% of alcoholic ammonia solution. The resulting solution was stirred for 3.5 hours at 70°C, followed by the concentration to one third of its volume. Fine amorphous colorless/colored product was obtained, which was iteratively washed with methanol and water. Before characterization all the metal complexes were dried overnight in hot air oven at 45^{o}C, then in vacuum desiccators for 3 days.

2.1.3 DFT Calculations

All density functional theory (DFT) static calculations were performed at the GGA level with Gaussian09 set of programs, using the BP86 functional of Becke and Perdew (Becke et al, 1988; Perdew et al. 1986)**.** The electronic configuration of the molecular systems was described with the triple zeta valence plus polarization, using TZVP keyword in Gaussian (Frisch et al. 2009). The geometry optimizations were performed without the symmetry constraints. For the studied ligand-metal complexes, Mg^{2+} was considered in singlet spin states. However, Cu^{2+}, Ni^{2+}, Mn^{2+} were considered in doublet, triplet and sextuplet spin states which correspond to their respective ground states. We carried out all the geometry optimizations using the PCM model with water as the solvent. The reported energies were optimized via single point energy calculations on BP86 geometries with again triple zeta valence plus polarization (TZVP) using M06 functional (Zhao et al. 2008). For estimating the solvent effects, polarizable solvation model PCM was used using water as solvent (Barone et al. 1998).

2.2. Biological Studies

2.2.1 Antimicrobial assays

The antibacterial activities of the investigated compounds were tested against six bacterial strains as given below with coding **1** to **6** as: **1**=*Streptomyces antibioticus,* **2**= *Pseudomonas putida,* **3**= *Bacillus brevis,* **4**=*Arthrobacter citreus,* **5**=*Escherichia coli,* **6**=*Salmonella typhimurium.* All the experiments were run in triplicates.

In vitro antibacterial studies were carried out by agar disc diffusion method against test organisms (Rex et al. 2007). Nutrient broth (NB) plates were swabbed with 24h old broth culture (100mL) of test bacteria. Sterile paper discs (5 mm) were put into each petriplate. Different concentrations of DMSO dissolved compounds (50, 125, and 250µg/L) were added into the discs by dipping individual disc into solution containing test tubes. DMSO was taken as negative control and chloramphenicol as positive control. The plates were incubated at 37^{o}C for 24h. After appropriate incubation, the diameter of zone of inhibition of each disc was measured.

2.2.1.1. MIC determination

MIC (µM) values were evaluated by using the serial double dilution method in the appropriate medium which is inoculated with a standardized number of microorganisms.

2.2.2. Antioxidant Activity

The antioxidant activity TCSA and its complexes were measured by using 1,1- diphenyl-2-picrilhydrazyl (DPPH) assay. 20, 40, 60, 80, and 100 µL of 100 ppm ethanolic solution of each compound were mixed with 4.0 mL of 0.1 mM ethanolic solution of DPPH. The mixture was shaken vigorously and left to stand for 30 min in the dark. The absorbance was then measured at 517.0 nm against a blank. The control was prepared, as above, without any

complex added. IC_{50} (Concentration of antioxidant to reduce the DPPH to its half concentration value) values were then calculated and reported.

2.2.3. Protein (BSA) interaction with TCSA and its metal chelates

The absorption spectra were recorded on a Shimadzu 1800S spectrophotometer, using a slit of 5.0 nm and a scan speed of 250 nm min^{-1} as described by Abdi et al. (2012) The UV absorption of BSA in presence and absence of product solutions were measured at pH 7.2 by keeping the concentration of BSA constant (0.05mM), while varying the concentration of the metal complex/ TCSA (5×10^{-3}, 12.5×10^{-3}, 25×10^{-3}, 37.5×10^{-3}, and 50×10^{-3}mM), in the range of 230–400 nm. The binding constants of the drug–BSA interaction were calculated by the method as reported (Abdi et al. 2012; Kumar et al. 2016).

3. Results and Discussion

3.1 Chemical Studies

The light essential metal ion complexes (till the first transition series) with TCSA ligand were synthesized at around neutral pH and washed in portions with methanol and water till the complete removal of unreacted ligand and metal ion from the precipitate. The formed products were characterized by various spectroscopic techniques, including CHN study, UV-vis, IR, NMR spectrophotometer and Mass spectrometer. In general, almost all metal complexes have shown a slight blue shift coupled with decrease in intensity of stretching of band associated with hydroxyl and carbonyl groups of TCSA has been predicted/ noted by comparative IR spectra (Kumar et al. 2015b). Interestingly, with the formation of metal-TCSA complexes, the stretching of carbonyl band, ν(C=O) of TCSA shifted from 1681 cm^{-1} to 1645-1670 cm^{-1}. The IR bands centered at 412–583 cm^{-1} indicate the presence of metal phenoxide (M–O) bond (See Figure 1). The presence of strong absorptions observed for all the complexes at 1595–1631 and 1380–1411 cm^{-1} resulted due to the asymmetric and symmetric vibrations of the COO moiety respectively. Notably, a strong absorption band/peak around 655 cm^{-1} for metal-TCSA complexes resulted because of the O–M–O (phenoxy-metal-carbonyl) stretching vibration. All these values are consistent with those detected in recent studies of TCSA metal complexes (Wang et al. 2013).

In the ^{1}H-NMR data of TCSA and its metal complexes with the expected integrations and peak multiplicities, all the metal complexes have shown three broad peaks between 6.0-9.0 ppm, assigned to the ring proton of the TCSA moiety and two non-equivalent coordinated water molecules.

From the mass spectra of the metal complexes, the dianionic TCSA ligand was confirmed to be coordinated with each metal ion, together with two additional water molecules, with m/z 335 to 720. Almost all metal complexes under study show the most intense peak at a position bearing one TCSA ligand with a metal ion and two water molecules. For example, in detriment of 338.2 m/z value of copper complex with TCSA (including two TCSA molecules, two water molecules and one Cu^{2+} ion) the most intense peak was observed at m/z 301.9 (one TCSA and one metal ion). The entire data is summarized below:

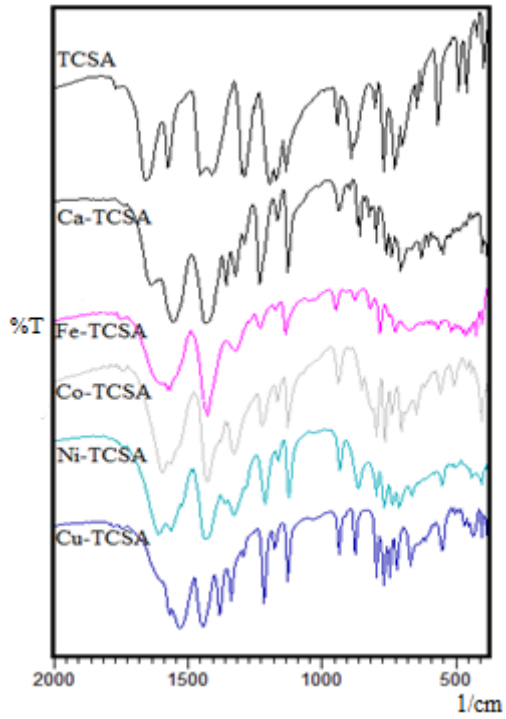

Figure 1: Comparative FTIR spectrum of metal complexes of TCSA.

TCSA (white); UV (MeOH) 295 and 315 nm; FTIR (KBr) 3473, 3081, 1681, 1577**,** 1482, 1200, 1177, 892, 771, 733, 716, 574, 490 and 460cm^{-1}; ^{1}H NMR (400 MHz, DMSO-d_6) δ 7.56 (s, 1H), δ 10-11 (b, 2H).

Mg(II)-TCSA (Dirty white; m.p. 223±2^{o}C; yield; 51.06%);UV (DMSO) 259, 335 and 423nm; FTIR (KBr) 3611, 1615, 1561, 1482, 1385, 1338, 1246, 1131, 869, 498 and 430cm^{-1}; ^{1}H NMR (400 MHz, DMSO-d_6) δ 7.73 (S, 1H), δ 17-19 (b, 1H).; ESI-MS calculated for [Mg(TCSA)(H_2O)$_2$]; 301.8, found: 301.8; Anal. Calcd.(Obs.), C - 27.94 (27.89), H – 1.64 (1.59).

Ca(II)-TCSA (Cream white; m.p. 236±2^{o}C; yield; 52.45%); UV (DMSO) 262, 325 and 436nm; FTIR (KBr) 3611, 1654, 1561, 1482, 1369, 1331, 1246, 1138, 869, 574 and 428cm^{-1}; ^{1}H NMR (400 MHz, DMSO-d_6) δ 7.68 (S, 1H); ESI-MS calculated for [Ca(TCSA)$_2$(H_2O)$_2$]; 317.6, found: 317.4; Anal. Calcd.(Obs.), C - 26.65 (27.05), H – 1.60 (1.64).

Mn(II)-TCSA (Puffy white; m.p. 282±2^{o}C; yield; 53.65%); UV (DMSO) 298, 325 and 584nm; FTIR (KBr) 3588, 1584, 1546, 1482, 1392, 1354, 1238, 1138, 848, 531 and 416cm^{-1}; ESI-MS calculated for [Mn(TCSA)(H_2O)$_2$]; 331.44, found: 332.1; Anal. Calcd.(Obs.), C - 25.36 (25.45), H – 1.52 (1.58).

Fe(II)-TCSA (Brown red; m.p. 294±2^{o}C; yield; 53.86%); UV (DMSO) 247, 321 and 487nm; FTIR (KBr) 3452, 1613, 1575, 1475, 1325, 1234, 1138, 861, 521 and 460cm^{-1}; ESI-MS calculated for [Fe(TCSA)(H_2O)$_2$]; 554.8, found: 555.7; Anal. Calcd.(Obs.), C - 25.29 (25.47), H – 1.52 (1.55).

Co(II)-TCSA (Light purple; m.p. 291±2^{o}C; yield; 54.12%); UV (DMSO) 218, 327 and 538nm; FTIR (KBr) 3567, 1600, 1569, 1479, 1331, 1223, 1138, 854, 523 and 416cm^{-1}; ESI-MS calculated for [Co(TCSA)(H_2O)$_2$]; 337.4, found: 338.3; Anal. Calcd.(Obs.), C - 24.99 (25.12), H – 1.55 (1.57).

Ni(II)-TCSA (Light green; m.p. 297±2^{o}C; yield; 54.11%); UV (DMSO) 297, 323 and 412nm; FTIR (KBr) 3578, 1615, 1569, 1484, 1338, 1223, 1131, 865, 570 and 431cm^{-1}; ESI-MS calculated for [Ni(TCSA)(H_2O)$_2$]; 336.2, found: 336.90; Anal. Calcd.(Obs.), C – 25.01 (25.02), H – 1.53 (1.54).

Cu(II)-TCSA (Brown; m.p. 293±2°C; yield; 55.16%); UV (DMSO) 298, 333 and 582nm; FTIR (KBr) 3484, 1661, 1569, 1531, 1473, 1346, 1223, 1131, 859, 521 and 430cm^{-1}; ESI-MS calculated for [Cu(TCSA)$_2$(H$_2$O)$_2$]; 582.5, found: 583.3; Anal. Calcd.(Obs.), C – 28.87 (29.01), H – 1.34 (1.35).

Zn(II)-TCSA (White; m.p. 235±2°C; yield; 52.16%); UV (DMSO) 299 and 321nm; FTIR (KBr) 3572, 1610, 1565, 1482, 1346, 1231, 1138, 855, 471 and 410cm^{-1}; ESI-MS calculated for [Zn(TCSA)(H$_2$O)$_2$]; 342.9, found: 343.9; Anal. Calcd.(Obs.), C – 24.52 (24.63), H – 1.47 (1.53).

Further, in situ proceedings of the reaction between TCSA and metal ions were also analyzed employing UV-vis spectral analysis. The decrease in the absorption bands were found at 295 and 315 nm with the increase in time due to the formation of solid product in reaction mixture and decrease of concentration of reactant. The products formed were also analyzed spectrophotometrically in DMSO in 200-600 nm range. The isolated TCSA possesses two distinct absorption bands at 295 nm and 315 nm. The former peak could be attributed to $\pi \rightarrow \pi^*$ intra-ligand transition of the aromatic ring, while the second corresponds to the $n \rightarrow \pi^*$ electronic transition. In contrast, for the metal complexed with TCSA, the two bands were hypsochromically affected, clearly suggesting the coordination of the TCSA molecule with the metal ions. In addition, a d-d transition band was also observed in the complexes, with peak positions varying from 410 nm to 700 nm, depending on the type of metal of the complex.

In order to confirm the above mentioned chemical features, and the associated stability of the metal bound ligand complexes, thermal analysis was carried out at the heating rates of 10°C/min starting from room temperature up to 850°C. Notably, all metal complexes were found to give almost similar trends of decomposition and the complete TGA/DSC pattern occurred in three steps. For example, degradation of iron complex [Fe(TCSA)(H$_2$O)$_2$] took place in the range of 35-110°C which corresponds to the elimination of two water molecules with an observed weight loss of 6.41% (calculated = 6.63%), the second degradation step falls in the range of 110-400°C which is assigned to the loss of TCSA molecules with a weight loss 89.36% (calcd. = 89.58%) and finally, between 400–800°C which resulted in the formation of metal-oxide (FeO) from FeCl$_2$.

The structures of the TCSA molecule complexed with different metal ions have been confirmed utilizing the FTIR, UV-Vis, ^{1}H-NMR, mass and thermal analysis data. From our analysis, it seems reasonable to conclude that TCSA behaves as a bidentate ligand coordinated to the metal ions via the oxygen atom of hydroxyl and carbonyl group. However, the structure of products was difficult to predict, because of the chances of either of survival of a carboxylic proton or a phenolic proton. Since it is well known that the carboxylic protons are highly acidic in nature, thus, should be removed before the removal of phenolic proton. To reinforce unravel whether the proton will be removed from the phenolic -OH group or from the –COOH moiety of the trichlorosalicyclic acid (TCSA), we carried out the detailed DFT investigations, where we modeled two possible structures (see Figure 2). First, we modeled the TCSA with a proton removed from the hydroxyl group, and next, the proton is removed from the carboxylic acid moiety, retaining the OH group.

Looking at the optimized geometries, see Figure 2, it is evident that the presence of a proton at the carboxylic acid moiety stabilizes the metal ligand complex by a quite strong H-bond between the O-H···Cl, see Figure 2. Further, a similar H-bond (O-H···Cl) is also possible for the other isomer where a phenolic proton is present. However, removing a proton

from the –COOH moiety, results in the repulsion between one of the oxygen atoms of the carboxylate group and its nearby electron rich chlorine atom, with simultaneous orientation of oxygen atom from carboxylate groups from the two coordinated ligands resulting in a H-bond with the metal coordinated water molecule. This apparently leads to the substantial deformation in the metal-ligand complexed geometries, see A′ and B′ in Figure 2. The geometry distortion, however, is more pronounced in the Cu^{2+} coordinated structure, even missing the H-bond with the metal coordinated water molecule.

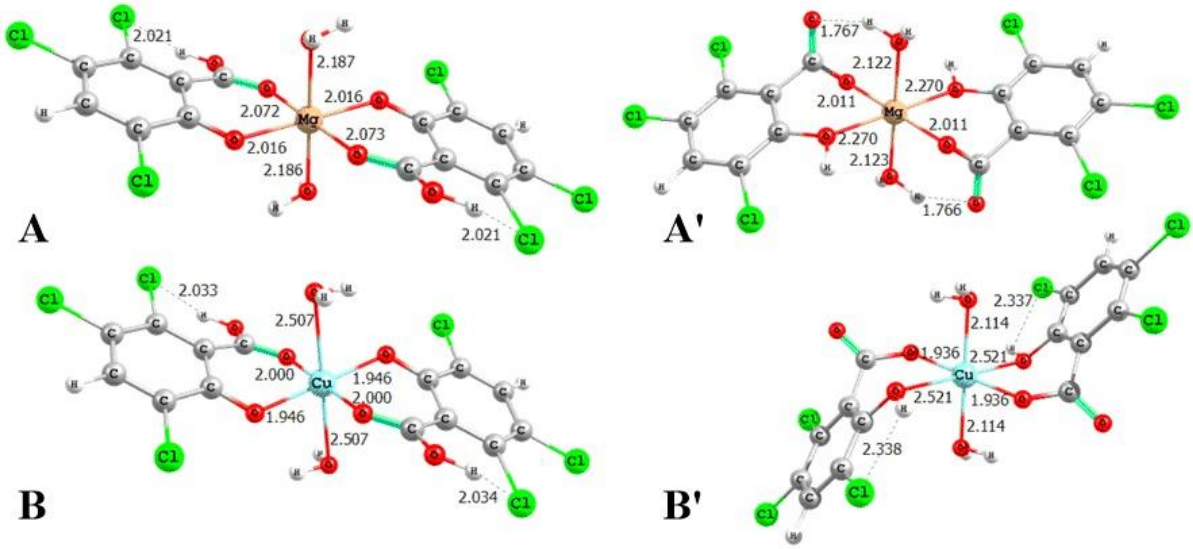

Figure 2: Optimized geometries for the modeled **2TCA-X**, where X = Mg^{2+} (A, A′) and X =Cu^{2+} (B, B′) with the two bidentated ligands coordinated in *trans*. A, B and A′, B′ represent the geometries with the proton retained at the carboxylic acid moiety, and the hydroxyl moiety, respectively (main distances in Å).

Next, the energetic data reveal that the structures possessing –COOH groups (A, B) are more stable by -6.34 and -5.67 kcal/mol for the Mg^{2+} and Cu^{2+}complexed with TCSA ligands respectively, clearly indicating the better stability of structures A, B, compared to A′ and B′ in Figure 2. Structurally, the Mg-O bonds for A differ by less than 0.2 Å, whereas for A′ goes up to nearly 0.4 Å, bearing two Mg-O distances that are at the limit of a bond. The Mayer Bond Orders (MBO) (Mayer et al. 1983) confirm the latter hypothesis with values of less than 0.01 for both Mg-O(H) bonds included in A′, thus enjoying a square planar metal geometry rather than the octahedral environment in A (Poater et al. 2011). The same conclusions are suitable for the isomer A′ for copper with both Cu-O(H) bonds bearing MBOs equal or lower than 0.05. However, a nearly square planar geometry is also valid for isomer A, where the M-OH_2 bonds bear MBOs lower than 0.15.

Finally, the CHNS experimental data point towards existence of most of the metal ions coordinated to a single ligand, together with two water molecules, possibly forming the tetrahedral or square planar complexes, which is supported by mass and ^{1}H- NMR spectral data. To investigate this, we further carried out the modeling and compared the relative stabilities of two ligands simultaneously coordinated to metal ions, together with two water molecules, achieving an octahedral geometry, versus, the coordination of a single ligand with the metal ions (Mg^{2+}, Cu^{2+}, Mn^{2+}, and Ni^{2+}), still in combination with the coordination of two water molecules again, displaying either square planar or tetrahedral geometry, (see Figure 3). For all the studied metal complexes, it has been observed that for a single ligand coordinated to the metal ion, square planar geometry is more favored energetically with respect to the tetrahedral geometry. Interestingly, our energetic data nicely supports the

experimental observation of the coordination of a single di-anionic ligand to the metal ions, bearing square planar geometry in all the studied cases, more stable than their corresponding octahedral geometries with free energy differences of -15.7 kcal/mol, -18.2 kcal/mol, -14.1 kcal/mol, and -23.6 kcal/mol for mono-di-anionic ligand coordinated to Mg^{2+}, Mn^{2+}, Ni^{2+} and Cu^{2+} ions respectively.

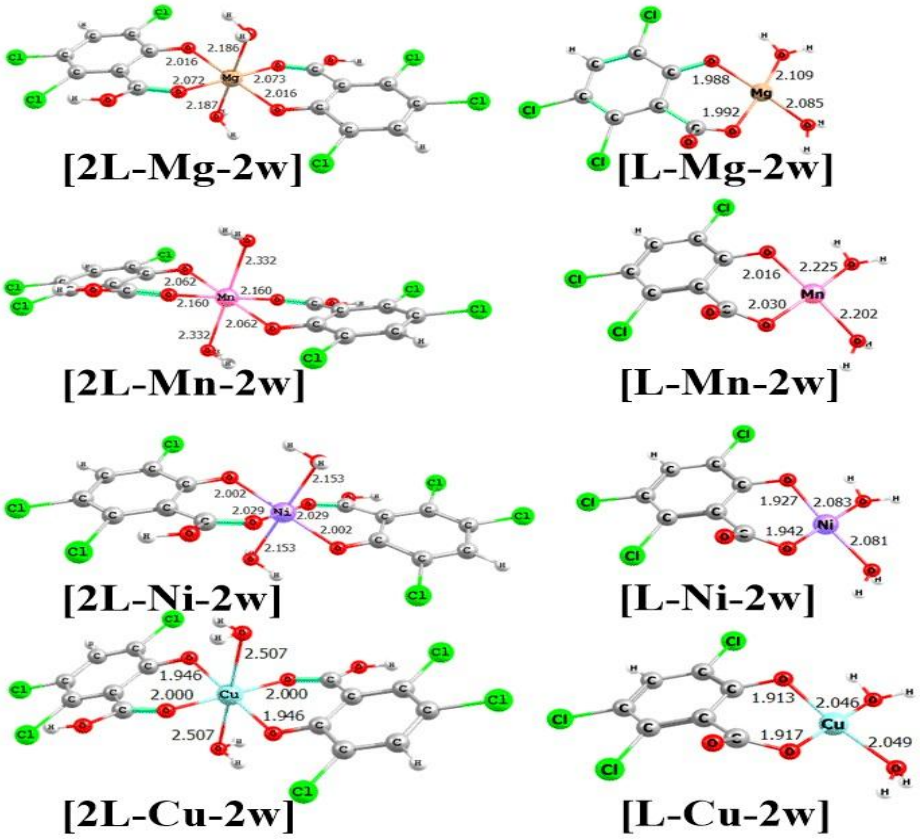

Figure 3: Optimized geometries of metal complexes with monoanionic TCSA and dianionic TCSA ligand. 'L' refers to a single dianionic TCSA ligand, whereas 2L refers to two monoanionic TCSA ligands coordinated to respective metal ions (main distances in Å).

It is well known that sterics may also play role in stabilizing the mono-coordinated TCSA ligand to the metal site, thus in order to better understand, we now calculated the sterical maps (see Figure 4). Focusing on the steric properties of the metal complexes bearing one or two TCSA ligands, we calculated the buried volume (%VBur) using the SambVca package developed by Cavallo et al. (Poater et al., 2016), since it provides information about the first coordination sphere around the metal. Actually, the buried volume is the amount of the first coordination sphere of the metal occupied by a given ligand. And here we plotted as well the steric contour steric maps in Figure 4 (Falivene et al., 2016). It is evident from Figure 4 that the studied metal complexes present quite similar sterics, thus the presence of a second TCSA ligand only increases the percent buried volume (%VBur) by 1.5% (%VBur for one and two TCSA ligands is 53.4% and 54.9%, respectively), since water molecules impose a similar sterical hindrance around the metal than the TCSA ligand.We performed also a more detailed analysis by evaluating the %VBur in the single quadrants around the metal center.Splitting the total %VBur into quadrant contributions quantifies any asymmetry in the way the ligand wraps around the metal. Bearing only one TCSA ligand, only a quadrant is highly sterically crowded (67.9%) due to the carboxylic moiety, with respect to the other less sterically hindered three quadrants, specially where the water ligands are placed (46.7% and 47.0%),

and for the oxo ligand the %VBur is 51.9%. On the other hand, bearing two TCSA ligands,imposes two highly sterically hindered quadrants around the metal (65.0% and 65.3%) due to the carboxylic moieties, with respect to the other two quadrants (44.7% and 44.8%). The results of this analysis clearly indicate that the studied metal complexes present quite similar sterics, pointing that sterics play a minimum role.

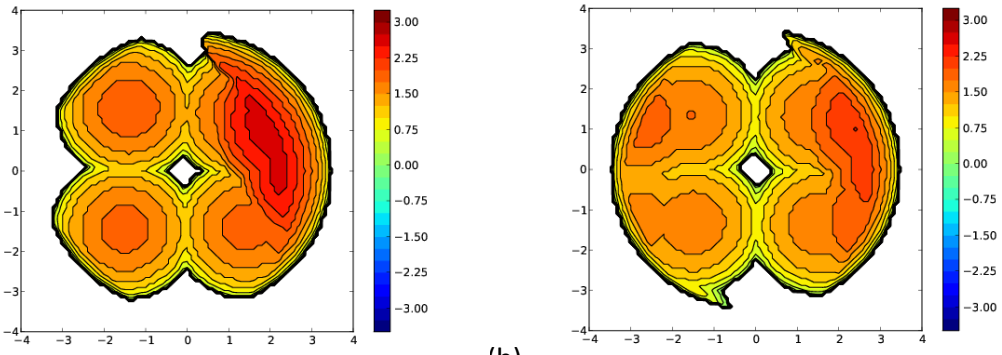

(a) (b)

Figure 4: Topographic steric maps of the NHC ligands for (a) L-Mg-2w and (b) 2L-Mg-2w. The metal is at the origin and the steric maps correspond to the plane XY that includes the metal and one and two TCSA ligands (the water molecules in the Z axis are excluded from the analysis), respectively. The isocontour curves of the steric maps are given in Å.

It has to be remarked that some of the metal ions like Mg(II), Ca(II) etc. have a strong preference towards the coordination number of six. However, a series of examples are well reported in literature where it is known that the Mg(II) also possesses the coordination number of four (Hallmen, 1995). Also, the coordination number of four for Mg(II) is well known for the chlorophyll molecule universally present in plant system.

SEM analyses indicated that the synthesized TCSA metal complexes had nanorods kind of structure with the size ranging from 120 to 260 nm (Figure 5). It has been already reported that nano sized compounds show enhanced biological/ medicinal activity with additional advantage of easy delivery, less time of action in biological system and least toxicity (Kumar et al. 2014; Masoomi et al. 2012 and Seil et al. 2012).The synthesized complexes were therefore thought to have high potential to act as medicinal drugs. To test their biological activity, antibacterial activity and interaction with BSA protein have been checked.

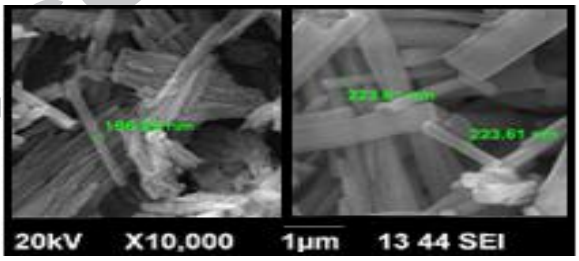

a) b)

Figure 5: SEM images of needle shaped nano sized TCSA-metal complexes: a) Fe-TCSA and b) Cu-TCSA.

3.2 Biochemical Studies

3.2.1 Antimicrobial activity

TCSA and its metal complexes have been tested for antibacterial activity at three different concentrations 50, 125 and 250 µg/L against six pathogenic bacterial strains using the disc

diffusion method. Further dilutions were done to perform the Minimal Inhibitory Concentration (MIC). If MIC value came between any two of the concentration written above, then it was further checked by dividing that range in multiple of 25 that too was further splitted at the multiple of 5 (µg/L) to minimize the number of test samples in the same manner and due to the same reason. The results of antibacterial activities of the metal complexes of TCSA (in micromolar for comparison) are presented in Table 1. Among the nine studied metal complexes Mg(II)-TCSA, Ca(II)-TCSA, Mn(II)-TCSA, Ni(II)-TCSA, Cu(II)-TCSA, and Zn(II)-TCSA were found to be biologically active over a range from 20 to 100µg/L.

One of the studied strains includes Streptomycetes that infects human beings and causes variety of infections, including mycetoma, hearing loss, renal toxicity and dizziness (Todar et al. 2007). The TCSA metal complexes bearing different metal centers viz. of Mg(II), Ni(II), Cu(II), and Zn(II) have been found to be more active than control (Chloramphenicol) and TCSA against *Streptomyces antibioticus* with an order: Zn(II) > Ni(II)> Mg(II)> Cu(II). Next, we studied another bacterial strain, *Pseudomonas putida* which is well known to cause urinary and respiratory tract infections (Rosenberger et al. 2000). Amongst all the studied complexes Zn(II)-TCSA has shown better activity against the *Pseudomonas putida strain*. Further, Mn(II)-TCSA complex has been found to possess excellent activity against the bacterial strain *Arthrobactercitreus*. It is well known that the *E. Coli* and *Salmonella typhimurium* species are the causative agents of typhoid fever and diarrheal infections in humans, and are responsible for an estimated 40 million cases of systemic typhoid fever worldwide each year (Mellor et al. 1985, Anaissie et al. 1987). In these cases, Fe(II)-TCSA was found active against*Escherichia coli* and Cu(II)-TCSA against *Salmonella typhimurium*with respect to the control (chloramphenicol).

Table 1: Antibacterial and Antioxidant (against DPPH) activities of TCSA and its metal complexes (**1**=Streptomyces antibioticus, **2**= Pseudomonas putida, **3**= Bacillus brevis, **4**=Arthrobactercitreus, **5**=Escherichia coli, **6**=Salmonella typhimurium. Values are based on a mean of triplicate experiments; NA = not applicable; ND = not determined).

Moiety	**Bacterial strains and activity in µM**							**AO Activity (IC_{50} in µM)**
	1	**2**	**3**	**4**	**5**	**6**	Average	
Chloramphenicol	0.38	0.19	0.31	0.15	0.14	0.15	0.22	ND
Ascorbic Acid	NA	NA	NA	NA	NA	NA	NA	8.46
TCSA	>1.04	0.73	0.52	>1.04	0.41	>1.04	0.79	4.10
Mg(II)-TCSA	0.25	>0.83	0.25	>0.83	0.50	>0.83	0.58	2.71
Ca(II)-TCSA	>0.79	>0.79	0.55	0.20	0.23	>0.79	0.55	2.37
Mn(II)-TCSA	>0.75	0.30	>0.75	0.07	0.45	>0.75	0.51	2.26
Fe(II)-TCSA	0.37	>0.74	>0.75	>0.75	0.11	>0.75	0.57	2.29
Co(II)-TCSA[a]	0.44	0.29	>0.74	0.22	>0.74	>0.74	0.53	2.39
Ni(II)-TCSA[a]	0.13	>0.74	>0.74	>0.74	>0.74	>0.74	0.63	2.45
Cu(II)-TCSA	0.36	0.29	>0.73	0.22	>0.73	0.15	0.41	2.18
Zn(II)-TCSA	0.10	0.14	>0.73	0.44	>0.73	>0.73	0.48	2.22

[a]partially soluble

The above analysis has clearly shown to serve as an important tool that could be specifically and selectively utilized to fight against the infections caused by various bacterial strains. New metal complexes of TCSA may help in controlling the increased rates of resistance of various harmful pathogens by acting against various pathogenic strains mentioned in **Table 1.** The average MIC values of antibacterial activity of each compound against six chosen bacteria were found in accordance with the antioxidant activity of the particular complex.Therefore, the antibacterial activity of the complexes seems to be related with its antioxidant activity.

3.2.2 BSA protein binding

TCSA and its metal complexes have been tested for protein binding at five different concentrations 5.0×10^{-3} to 50.0×10^{-3} mM (5.0×10^{-3}, 12.5×10^{-3}, 25.0×10^{-3}, 37.5×10^{-3}, and 50.0×10^{-3} mM) with BSA. An increase in the concentrations resulted in an increase in UV light absorption and shifting of BSA band from 279 nm to 274 nm that can be indicative of the complex formation. The binding constants of the complexes were determined by using UV–vis spectroscopic method. The double reciprocal plot of $1/(A-A_0)$ versus 1/(ligand concentration) was found linear and the binding constant (k) was determined from the ratio of the intercept to the slope. The exact order of protein binding constant was found to be Ca(II)-TCSA >> Cu(II)-TCSA > Mg(II)-TCSA >>Mn(II)-TCSA >> Zn(II)-TCSA >>>> Ni(II)-TCSA >>> Co(II)-TCSA > Fe(II)-TCSA > TCSA (Table 2). All these results may suggest a medium affinity of metal complexes for BSA interaction, when compared to a weak interaction of TCSA-BSA complex. It is well known that the molecules with binding constants ranging from $10^6\ M^{-1}$ to $10^8\ M^{-1}$ could be considered to possess strong binding with BSA. The observed interaction of a drug with BSA protein lies in between the weak and strong interaction of drug with BSA protein (Kragh-Hansen, 1990 and Liu et al. 2004).

Further, it is known that value of binding constant of TCSA ($1.54\times10^4 M^{-1}$) is almost similar to that of salicylic acid ($1.89\times10^4\ M^{-1}$), but is significantly different from 5-chlorosalicylic acid ($6.11\times10^2 M^{-1}$)(Archibaldet al. 2013). Next, it is also well known that the metal complexes of the drugs have been found to possess significant influence on protein-binding properties, because of complex shape and coordination preferences of the metal ion (donor type and geometry) (Barone et al. 1998; Rex et al. 2007; Tomasi et al. 1994). The effect of metal complexes of TCSA was corroborated with the same fact. It was interesting point of our study that essential and least toxic metal ions such as Ca(II), Co(II), Cu(II) and others have shown a considerable binding affinity with BSA protein as compared to TCSA, salicylic acid and 5-chlorosalicylic acid (**Table 2**).

Table 2: Interaction with BSA protein of TCSA and its metal complexes

Moiety	**BSA interaction k (M^{-1})[a]**	**Moiety**	**BSA interaction k (M^{-1})[a]**
TCSA	$1.54\ (\pm0.08)\times10^4$	Co(II)-TCSA	$1.98\ (\pm0.09)\times10^5$
Mg(II)-TCSA	$7.51\ (\pm0.05)\times10^5$	Ni(II)-TCSA	$2.73\ (\pm0.06)\times10^5$
Ca(II)-TCSA	$9.53\ (\pm0.07)\times10^5$	Cu(II)-TCSA	$8.47\ (\pm0.05)\times10^5$
Mn(II)-TCSA	$5.38\ (\pm0.15)\times10^5$	Zn(II)-TCSA	$5.36\ (\pm0.08)\times10^5$
Fe(II)-TCSA	$1.88\ (\pm0.12)\times10^4$		

[a]Values are based on a mean of triplicate experiments

4. Conclusions

Eight distinct metal complexes bearing TCSA as a ligand were synthesized and characterized. The resolution of ambiguity of the structural nature was performed by DFT

calculations. It has been observed that the complexes bearing TCSA seem to possess energetically favoured square planar geometry as compared to octahedral geometry, together with the fact that unlike other metal-SA complexes, here phenolic group is releasing its proton prior to carboxylic group during complex formation. The studied metal complexes of TCSA have displayed considerable antibacterial activities, which were found related with the antioxidant activity of the complexes. Further, it is observed that the different metal chelates of TCSA involving metals such as, Fe(II), Cu(II) and Zn(II) could act as potential antibacterial agent. The activity of the complex against different microbes was not found identical and therefore for a fixed purpose an individual drug can be used. The minimum MIC values for metal complexes were found in a range of 20-75 ppb and for every microbe (out of six studied), All the studied metal complexes were found potential protein binders compared to the free ligand TCSA. The exact order of the protein binding constant was found in the order: Ca(II)-TCSA >>Cu(II)-TCSA > Mg(II)-TCSA >>Mn(II)-TCSA >> Zn(II)-TCSA >>> Ni(II)-TCSA > Co(II)-TCSA > Fe(II)-TCSA > TCSA and in a range of 1.5×10^4 to 8.9×10^5 M^{-1}. Moreover, the synthesized metal complexes enjoy nanosize (between 120 to 260 nm) and therefore expected to show relatively better biological activity than TCSA itself.

Abbreviations:
SA: Salicylic acid
TCSA: 3,5,6-Trichlorosalicylic acid
Mg(II)-TCSA: diaqua-3,5,6-trichlorosalicylatomagnessium(II)
Ca(II)-TCSA: diaqua-3,5,6-trichlorosalicylatocalcium(II)
Mn(II)-TSA: diaqua-3,5,6-trichlorosalicylatomangnese(II)
Fe(II)-TCSA: diaqua-3,5,6-trichlorosalicylatoiron(II)
Co(II)-TCSA: diaqua3,5,6-trichlorosalicylatocobalt(II)
Ni(II)-TCSA: diaqua-3,5,6-trichlorosalicylatonickel(II)
Cu(II)-TCSA: diaqua-3,5,6-trichlorosalicylatocopper(II)
Zn(II)-TCSA: diaqua-3,5,6-trichlorosalicylatozinc(II)
DPPH: 1,1- diphenyl-2-picrilhydrazyl
DMSO: Dimethylsulfoxide
IR: Infrared
FTIR: Fourier Transform Infrared
NMR: Nuclear Magnetic Resonance
MIC: Minimum Inhibitory Concentration
IC_{50}: Half Maximal Inhibitory Concentration
E. Coli: Escherichia coli
BSA: Bovine serum albumin
HSA: Human serum albumin
SEM: Surface electron microscope
DFT: Density Functional Theory
TZVP: Triple zeta valence plus polarization
PCM: Plarizable solvation model
MBO: Mayer Bond Orders

Acknowledgements
This work is supported (finically) by UGC, India through UGC- start-up grant provided to Dr. Niraj Upadhyay (No. F. 30-70/2014) and by Rajiv Gandhi National Fellowship scheme awarded to Mr. Vijay Kumar (RGNF-SCHIM-1223). Authors also like to acknowledge SAIF, Punjab University Chandigarh and SAIF, Kerala University Kochi for the provision of instrument facilities. Dr. AlbertPoater thanks the Spanish MINECO for a project CTQ2014-59832-JIN. Sr. Mohit Chawla and Prof.

Luigi Cavallo thank King Abdullah University of Science and Technology (CFF project) for support.

References

1. Abdi, K., Nafisi, S.H., Manouchehri, F.,Bonsaii, M., and Khalaj, A. (2012). Interaction of 5-fluorouracil and its derivatives with bovine serum albumin. *J. Photochem. Photobiol. B.* 107, 20-26.
2. Anaissie, E., Fainstein, V., Miller, P.,Kassamali, H.,Pitlik, S., Bodey, G.P.,and Rolston, K. (1987). Pseudomonas putida. *Am. J. Med.*82, 1191-1194.
3. Archibald S.J., and Smith, R. (2013). Protein-binding metal complexes: noncovalent and coordinative interactions. Comprehensive Inorganic Chemistry II (Second Edition), From elements to applications, bioinorganic fundamentals and applications: metals in natural living systems and metals in toxicology and medicine, 661-682.
4. Barone, V., and Cossi, M. (1998). Quantum calculation of molecular energies and energy gradients in solution by a conductor solvent model *J. Phys. Chem. A*102, 1995–2001; Tomasi J.,and Persico, M. (1994).Molecular interactions in solution: an overview of methods based on continuous distributions of the solvent. *Chem. Rev.*94, 2027-2094.
5. Becke, A. (1988). Density-functional exchange-energy approximation with correct asymptotic behavior. *Phys. Rev. A* 38, 3098-3100.
6. Brumas, V.,Brumas, B., and Berthon, G.(1995). Copper(II) interaction with nonsteroidal antiinflamatory agents. I. Salicylic acid and acetylsalicylic acid.*J. Inorg. Biochem.* 57, 191-207.
7. Brumas, V., Miche, H., and Fiallo, M. (2007). Copper(II) interaction with 3'5-diisopropylsalicylic acid (Dips): New insight on its role as a potential ·OH inactivating ligand. *J. Inorg. Biochem.*101, 565-577.
8. Falivene, L., Credendino, R.,Poater, A., Petta, A., Serra, L., Oliva, R., Scarano, V., and Cavallo, L. (2016). SambVca 2. A Web Tool for Analyzing Catalytic Pockets with Topographic Steric Maps. *Organometallics*35, 2286–2293.
9. Frisch, M.J., Trucks, G.W., Schlegel, H.B.,Scuseria, G.E., Robb, M.A., Cheeseman, J.R., Scalmani, G., Barone, V., Mennucci, B., Petersson, G.A., Nakatsuji, H., Caricato, M., Li, X., Hratchian, H.P., Izmaylov, A.F., Bloino, J., Zheng, G., Sonnenberg, J.L.,Hada, M., Ehara, M., Toyota, K., Fukuda, R., Hasegawa, J., Ishida, M., Nakajima, T., Honda, Y., Kitao, O.,Nakai, H.,Vreven, T., Montgomery Jr., J.A., Peralta, J.E.,Ogliaro, F.,Bearpark, M.,Heyd, J.J., Brothers, E.,Kudin, K.N.,Staroverov, V.N., Kobayashi, R., Normand, J.,Raghavachari, K., Rendell, A.,Burant, J.C.,Iyengar, S.S.,Tomasi, J.,Cossi, M.,Rega, N.,Millam, J.M.,Klene, M., Knox, J.E., Cross, J.B., Bakken, V.,Adamo, C., Jaramillo, J.,Gomperts, R.,Stratmann, R.E.,Yazyev, O., Austin, A.J.,Cammi, R.,Pomelli, C.,Ochterski, J.W., Martin, R.L.,Morokuma, K.,Zakrzewski, V.G.,Voth, G.A., Salvador, P., Dannenberg, J.J.,Dapprich, S., Daniels, A.D.,Farkas, Ö.,Foresman, J.B., Ortiz, J.V.,Cioslowski J., Fox, D.J. Gaussian 09, Gaussian, Inc., Wallingford CT, 2009.
10. Hallmen, A.F., and Wiberg, E. (1995). Inorganic Chemistry, 1st English Edition by Nils Wiberg, Academic Press (New York), pp 1062.
11. Kantouch, A., El-Sayed, A.A., Salama, M., El-Kheir, A.A., and Mowafi, S. (2013). Salicylic acid and some of its derivatives as antibacterial agents for viscose fabric.*Int. J. Biol. Macromol.*62, 603-607.

12. Kaur, S.P., Kumar, V., Chawla, M., Cavallo, L., Upadhyay, N. (2017). Pesticide curbing soil fertility: effect of complexation of free metal ion. *Front. Chem.* 5:43.
13. Kragh-Hansen, U. (1990). Structure and ligand binding properties of human serum albumin *Dan. Med. Bull.*37, 57-84.
14. Kumar, N., and Kumar, R. (2014). Nanotechnology and nanomaterials in the treatment of life-threatening diseases. Chapter 2 – Nano-based drug delivery and diagnostic systems, Elsevier Inc. William Andrew Publisher. 53, http://dx.doi.org/10.1016/B978-0-323-26433-4.00002-6.
15. Kumar, V., Upadhyay, N., and Manhas, A. (2015a). Designing, syntheses, characterization, computational studies and biological activities of silver-phenothiazine metal complex.*J. Mol. Struct.* 1099, 135-141.
16. Kumar, V., Kumar, V., Upadhyay, N., Sarma, S. (2015b). Interaction of atrazine with transition metal ion in aqueous media: experimental and computational approach. *3Biotech* 5, 791-798.
17. Kumar, V., Kaur, S.P., Singh, S.,and Upadhyay, N. (2016). Unexpected formation of N'-phenyl-thiophosphorohydrazidic acid O,S-dimethyl ester from acephate: chemical, biotechnical and computational study. *3Biotech* 6(1), 1-11.
18. Li, Z.M., Wei, C.W., Zhang, Y., Wang, D.S., and Liu, Y.N. (2011). Investigation of competitive binding of ibuprofen and salicylic acid with serum albumin by affinity capillary electrophoresis. *J. Chromatogr. B* 879, 1934-1938.
19. Liu, J., Tian, J., and Hu, Z. (2004). Binding of isofraxidin to bovine serum albumin. *Biopolymers* 73, 443-450.
20. Mayer, I. (1983). Charge, bond order and valence in the AB initio SCF theory. *Chem. Phys. Lett.*97, 270-274.
21. Masoomi, M.Y.,andMorsali, A. (2012). Applications of metal–organic coordination polymers as precursors for preparation of nano-materials. *Coord. Chem. Rev*. 256, 2921-2943.
22. Mellor, J.A., Kingdom, J., Cafferkey, M.,and Keane, C.T. (1985). Vancomycin toxicity: a prospective study. *J. Antimicrom. Chemother.*15, 773-780.
23. Perdew, J.P. (1986). Density-functional approximation for the correlation energy of the inhomogeneous electron gas. *Phys. Rev. B* 33, 8822-8824; Perdew, J.P. (1986). Erratum: Density-functional approximation for the correlation energy of the inhomogeneous electron gas. *Phys. Rev. B* 34, 7406–7406.
24. Perrin, D.D. (1958). Stability of metal complexes with salicylic acid and related substances, *Nature* 182, 741-742.
25. Poater, A., Cosenza, B., Correa, A., Giudice, S., Ragone, F., Scarano, V., andCavallo, L. (2009). SambVca: A Web Application for the Calculation of Buried Volumes of N-Heterocyclic Carbene Ligands.*Eur. J. Inorg. Chem.* 1759–1766.
26. Poater, A., Ragone, F., Correa, A., and Cavallo, L. (2011). Comparing Ru and Fe-Catalyzed Olefin Metathesis. *Dalton Trans.*40, 11066-11069.
27. Rex, J.H., Alexender, B.D., Andes, D.,Arthington-Skaggs, B., Brown, S.D.,Chaturvedi, V.,Ghannoum, M.A.,Espinel-Ingroff, A., Knapp, C.C., Ostrsky-Zeichner, L., Pfaller, M.A., Sheehan, D.J., and Walsh, T.J.(2007). Reference method for broth dilution antifungal susceptibility testing of yeasts, approved standard—Third Edition M27-A3, 0 (0), Replaces 22 (15), M27-A2; Murray, P.R., Baron, W.J., Jorgensen, J., and Pfaller, M.L. (2007). Manual of Clinical Microbiology. Ninth ed., ASM Press, Washington.
28. Rosenberger, C.M., Scott, M.G., Gold, M.R., Hancock, R.E.W., and Finlay, B.B. (2000). *Salmonella typhimurium* infection and lipopolysaccharide stimulation induce similar changes in macrophage gene expression. *J. Immunol.*164, 5894-5904.

29. Seil, J.T., and Webster, T.J. (2012).Antimicrobial application of nanotechnology: methods and literature *Int. J. Nanomed.*7, 2767-2781.
30. Shi, L., Ge, H.M., Tan, S.H., Li, H.Q., Song, Y.C., Zhu, H.L., and Tan, R.X. (2007). Synthesis and antimicrobial activities of Schiff bases derived from 5-chloro-salicylaldehyde. *Eur. J Med. Chem.* 42, 558-564.
31. Todar, K. (2007). "Pathogenic E. coli". Online Textbook of Bacteriology. University of Wisconsin–Madison Department of Bacteriology. 11.
32. Wang, Q.-F, Ma, C.-L., He, G.-F, and Li, Z. (2013). Synthesis and characterization of new tin derivatives derived from 3,5,6-trichlorosalicylic acid: Cage, chain and ladder X-ray crystal structures. *Polyhedron* 49, 177–182.
33. Wani, A.B., Singh, J., Upadhyay, N. (2017a). Synthesis and characterization of transition metal complexes of para-aminosalicylic acidwith evaluation of their antioxidant activities. *Orient. J. Chem.*, 33(3), 1120-1126.
34. Wani, A.B., Chadar, H., Wani, A.H., Singh, S., and Upadhyay, N. (2017b). Salicylic acid to decrease plant stress. *Environ. Chem. Lett.* 15(1), 101-123.
35. Yin, T., Wei, W., Yang, L., Liu, K., Gao, X. (2007). Kinetics parameter estimation for the binding process of salicylic acid to human serum albumin (HSA) with capacitive sensing technique. *J. Biochem. Biophys. Methods* 70, 587–593.
36. Zhao, Y., and Truhlar, D.G. (2008). The M06 suite of density functionals for main group thermochemistry, thermochemical kinetics, noncovalent interactions, excited states, and transition elements: two new functionals and systematic testing of four M06-class functionals and 12 other functionals. *Theor. Chem. Acc.*120, 215-241.

Highlights:

- First time reporting synthesis and characterization of eight different (essential) metal complexes of trichlorosalicylic acid
- Metal complexes of trichlorosalicylic acid have shown better antibacterial activity than trichlorosalicylic acid
- The average MIC values of metal complexes against six studied bacteria were found to be related with their antioxidant activities
- The studied compounds have been found to show an average protein binding ability (neither weak, nor strong interaction with BSA protein)
- The resolution of ambiguity of the structures was performed by the theoretical DFT calculation
- All the formed complexes seem to possess the square planar geometry rather than octahedral or tetrahedral

Graphical Abstract: